



**HAL**  
open science

## Mesures des propriétés statiques et dynamiques des noyaux : utilisation de champ magnétique

G. Neyens

► **To cite this version:**

G. Neyens. Mesures des propriétés statiques et dynamiques des noyaux : utilisation de champ magnétique. École thématique. Ecole Joliot Curie "Noyau, champ et cortège", Maubuisson, (France), du 13-18 septembre 1999 : 18ème session, 1999. cel-00654185

**HAL Id: cel-00654185**

**<https://cel.hal.science/cel-00654185v1>**

Submitted on 21 Dec 2011

**HAL** is a multi-disciplinary open access archive for the deposit and dissemination of scientific research documents, whether they are published or not. The documents may come from teaching and research institutions in France or abroad, or from public or private research centers.

L'archive ouverte pluridisciplinaire **HAL**, est destinée au dépôt et à la diffusion de documents scientifiques de niveau recherche, publiés ou non, émanant des établissements d'enseignement et de recherche français ou étrangers, des laboratoires publics ou privés.

**MESURES DES PROPRIETES STATIQUES ET DYNAMIQUES DES NOYEAUX :  
UTILISATION DE CHAMP MAGNETIQUE**

GERDA NEYENS

*University of Leuven  
Instituut voor Kern- en Stralingsfysica  
Celestijnenlaan 200 D  
B-3001 Leuven  
Belgium*

**RESUME**

Dans ce cours, on donne d'abord les principes de base pour mesurer les moments statiques dipolaire et quadripolaire des états nucléaires ayant un temps de vie de moins d'une seconde. Les interactions utilisées pour ces mesures, sont l'interaction du spin du noyau avec un champ magnétique et avec un gradient de champ électrique induit par un cristal dans lequel les noyaux sont implantés. Les principes des mesures sont identiques pour les états fondamentaux et isomériques. Dans un deuxième cours, on donne une description formelle du principe de la mécanique quantique sur lequel une famille de ces techniques expérimentales est basée : le principe de mélange des niveaux nucléaires. Pendant les 10 dernières années, plusieurs techniques ont été développées basées sur ce principe, chacune avec sa propre région d'application.

**ABSTRACT**

In this course we give first some basic principles for measuring the static magnetic dipole and electric quadrupole moments of short-lived nuclear states using magnetic fields and electric field gradients in crystals. The principles are similar for isomeric states and ground states. The upper lifetime limit of the nuclear states that can be investigated using these experimental techniques is of the order of a second. In a second lecture, we will give a more formal description of the quantum mechanical principle which is behind one family of techniques: the nuclear level mixing principle. Based on this principle, various experimental techniques have been developed over the last 10 years, each having its own regions of applicability. Some examples will be given.

## I. INTRODUCTION

Why measure nuclear moments?

To understand the structure of nuclei, one can measure several parameters. The most obvious and first parameters to measure are the nuclear decay schemes, excited level schemes, lifetimes, and masses. With this information, one can find out already a lot about the structure of the nucleus. If the excited levels follow a rotational band it means that the nucleus is deformed and the level spacing gives a measure for the amount of deformation. Other nuclei near closed shells have the typical level scheme in which the pairing interaction becomes visible. One can try to reproduce the level scheme using large-scale shell model calculations. Comparison of model calculations to experimental results can reveal information on pairing interactions, proton-neutron interaction, etc. However, to get a clear insight into the single particle structure or the collective nature of nuclear states, static nuclear moments are crucial. The magnetic moment is sensitive to the single particle nature of the valence nuclei, while the nuclear quadrupole moment is sensitive to the collective nature. Some 15-25 years ago, many nuclear moments of radioactive nuclei have been measured, both in the ground state and in isomeric states <sup>1)</sup>. All of these nuclei were situated close to the line of stability, mainly on the neutron deficient side: they were produced mostly in fusion-evaporation reactions. Nice trends have been found, for example in the Pb-region were a strong increase of the quadrupole moment is found when neutrons are removed from the N=126 shell closure <sup>2)</sup>, while the magnetic moment is hardly changing with neutron or proton number. This was for example an indication that the N=126 neutron core is very soft and easy to deform, mainly due to the presence of the  $\nu 3p_{1/2}$  orbit near the Fermi surface.

Since a few years, there is a renewed interest to measure nuclear moments. This is because it has now become possible to produce and select very exotic nuclei, which are approaching more and more the borders of nucleon stability. Fascinating new features have been discovered, the most popular one is the existence of 'halo' structures in nuclei with a very asymmetric proton-to-neutron ratio <sup>3)</sup>. But also the appearance and disappearance of magic numbers: N=20 seems no longer magic for nuclei with 10-12 protons <sup>4)</sup>, N=40 is maybe a new magic number for nuclei with Z=28 <sup>5)</sup>, etc. And many other regions still remain to be discovered or better understood. To get a clear insight into the nature of these nuclei far from stability, nuclear moments are a crucial test for the existing and newly developed models. While dynamic moments are sometimes easier to measure (via lifetimes), they do not always

provide sufficient information, because they depend both on the initial and final state configuration. So, to get unambiguous information, for example on the structure of an isomeric state, or on the effective charges to calculate moments (dynamic or static), knowledge of static dipole and quadrupole moments is crucial, especially in nuclei where several shapes are coexisting.

In this course, I will focus on some techniques, which allow studying the static nuclear moments of short-lived nuclear states (10 ns – 1 s). Remark that the techniques presented here are complementary to the techniques based on the hyperfine interaction between the electronic and nuclear spin, as presented by F. Leblanc. The latter are applicable mainly for long-lived nuclei ( $\tau > 10$  ms), so in general to ground states. In the techniques discussed here, the nuclear magnetic dipole moment is studied via its interaction with a magnetic field, the electric quadrupole moment via its interaction with an electric field gradient. These interactions are applied on nuclei that are implanted into a stopper:

- \* a static magnetic field is provided by mounting a magnet around the stopper
- \* an electric field gradient is induced by choosing a proper crystal as stopper
- \* a radio-frequency (RF) magnetic field is induced by an RF-coil mounted around the stopper.

Each of these interactions can furthermore be combined, and will give rise to different types of techniques to measure nuclear moments. In the first part of the course, some general features of different techniques will be discussed and compared. A common feature is the need to have the nuclear spins oriented in space, the modification of this orientation due to some interactions, and the detection of the change of the spin-orientation via the anisotropy of the radioactive decay. Each step will be discussed briefly. In the second part of the course, I will discuss more detailed a technique which combines the two static interactions, causing mixing of nuclear hyperfine levels. This mixing induces a resonant change in the orientation of the ensemble spin, which is reflected in a change of the anisotropy of the radioactive decay. The anisotropy change will be a signature from which nuclear moments can be derived. The formalism to calculate the influence of the nuclear level mixing on the spin-orientation of the ensemble will be discussed.

## II. BASIC PRINCIPLES TO MEASURE MOMENTS OF SHORT-LIVED NUCLEI

### II.1. Production and selection of short-lived activity

If one wants to investigate the properties of short-lived nuclear states (lifetimes up to a few seconds), the first thing to consider is how to produce the (ground or isomeric) state of interest. As lifetimes are short, the nuclei of interest have to be transported to the experimental station in a very short time.

Several experimental conditions can be considered:

- *In-beam experiments using fusion-evaporation reaction*: the experiment happens at the production site, allowing the study of very short-lived (ns) high-spin isomers. The advantage of using a fusion-evaporation reaction <sup>6)</sup> is that a high amount of spin-alignment is obtained by the reaction itself (see further). However the reaction allows only production of nuclei at the neutron deficient side of the chart of nuclei. The disadvantage of in-beam experiments is that the recorded gamma spectra contain all the gammas produced in the reaction and spectra are very dirty. It is almost impossible to study very weakly produced isomers in such conditions; only yrast states of nuclei not too far from stability are easy. Some purification techniques can be applied, for example by using a pulsed beam and recording data only during the beam-off period.
- *On-beam experiments*: this term is used for experiments that are performed after the nuclei of interest have been separated from the other activities produced in the reaction. The big advantage of these on-beam experiments is that the radioactive nuclei of interest, which are often a very small fraction of all produced activity, can be separated from the rest and investigated in very clean conditions. This allows measurements on very rarely produced nuclear states (such as far from stability nuclei). The two main techniques to obtain this separation are the ISOL separation (Isotope Separator On-Line) <sup>7)</sup> and the recoil mass separation <sup>8)</sup>. Several ISOL separation techniques have been developed over the last 20 years in combination with different production mechanisms. Typical separation times are of the order of tens of ms, which mean that mainly ground states are investigated by this technique. In-flight mass separation after an intermediate energy fragmentation reaction is much faster, and allows also the selection of short-lived (down to 100 ns) isomeric states <sup>9)</sup>. The advantage of the fragmentation with in-flight mass separation, is that the spin-orientation induced by the fragmentation process, is maintained during the transport of the nuclei through the mass spectrometer, mainly because the nuclei are produced fully stripped <sup>10)</sup>.

## II.2. Orientation of the nuclear spins: the density matrix

The methods to measure static moments using the interaction with electromagnetic fields are all based on measuring a change of the spin-orientation of the nuclear ensemble. This means that some amount of spin-orientation has to be present at the time the nuclear spins start to interact with the applied fields. Before mentioning how this spin-orientation can be obtained, we first will define the different types of spin orientation as well as how this can be expressed in a formal way.

An ensemble of nuclei is called spin-oriented if the nuclear spins have a preferential direction in space. By defining a Z-axis, one can describe the spin-orientation with respect to this axis by the probability  $p_m$  that the nuclear spin has a projection  $|m\rangle$  onto this axis. This implies that an axial symmetry exists around this Z-axis, which is called the  $Z_{or}$  axis (figure 1). For a non-axial symmetric spin-orientation, the density matrix formalism has to be used to describe the orientation:

$$\rho_{mm} = \langle m | \rho | m \rangle$$

with the diagonal elements  $\rho_{m,m} = p_m$  the population of the different spin-projections and the non-diagonal elements describing the coherence between different m-states. This density matrix is related to the density tensor  $\rho_k^n$  <sup>(1)</sup>:

$$\rho_k^n = \sqrt{2k+1} \sum_m (-1)^m \begin{pmatrix} 1 & 1 & k \\ -m & m & 0 \end{pmatrix} \langle m | \rho | m \rangle \quad (1)$$

and to the orientation tensor  $B_k^n = \sqrt{2I+1} \rho_k^n^*$ .

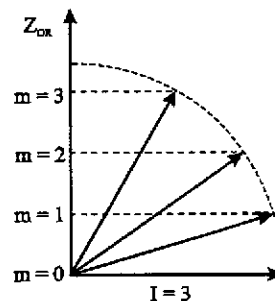


Figure 1: The projection of the nuclear spin  $I$  on a chosen Z-axis is defined as  $m$ . If  $p_m$  represents the probability to have the nuclear spin oriented such that they have spin-projection  $m$  on the  $Z_{or}$  axis, this means that this  $Z_{or}$  is an axial symmetry axis of the spin orientation.

The 3J-symbol in the relation between the density matrix and the tensor relates the values of the spin-projection and the tensor component  $n$ :  $m-m'=n$ . From this selection rule one can derive immediately that in case of axial symmetry (when only the diagonal elements are non-zero, or  $m=m'$  in the density matrix) the orientation tensor will only contain  $n=0$  components. This simplifies the description of an axially symmetric oriented system to a few parameters. In the angular distribution (see further) the spin-orientation will always be described by the orientation tensor, because it allows to easily transform the distribution function from one axis-system to another by rotation over the Euler angles<sup>12)</sup>. However, when speaking about the amount of orientation, people tend to use a different terminology, depending on the type of orientation (alignment or polarization). These terms are however related to some of the tensor components, as is explained hereafter.

### II.2.a. Alignment of nuclear spins.

An ensemble of spins is called *aligned* if the probability to have the spins along the axial symmetry axis is equal for both directions:  $p_m = p_{-m}$  (figure 2). The nuclear alignment is proportional to  $\sum_m (3m^2 - I(I+1))p_m$  and is directly related to the second order orientation tensor<sup>12)</sup>:

$$\begin{aligned} B_2^0 &= \sqrt{2I+1}\sqrt{5} \sum_m (-1)^{I+m} \begin{pmatrix} I & I & 2 \\ -m & m & 0 \end{pmatrix} p_m \\ &= \frac{\sqrt{5}}{\sqrt{I(I+1)(2I+3)(2I-1)}} \sum_m [3m^2 - I(I+1)] p_m \end{aligned} \quad (2)$$

The normalized alignment  $A$  is defined such that  $A = -1$  for full oblate alignment, and  $A=+1$  for full prolate alignment:

$$A \equiv \frac{\sum_m \alpha_2(m) p_m}{|\alpha_2(\max)|} = \frac{\sum_m (3m^2 - I(I+1)) p_m}{|\alpha_2(\max)|} \quad (3)$$

with  $\alpha_2(\max)$  the normalization value. For maximum *oblate alignment*, all spins are oriented perpendicular to the Z-axis ( $A < 0$ ), and maximum alignment  $A=-1$  is obtained if  $\alpha_2(\max)$  is:

$$\begin{aligned} |\alpha_2(m=0)| &= I(I+1) && \text{for integer spin,} \\ |\alpha_2(m=\pm 1/2)| &= I(I+1)-3/4 && \text{for half integer spin.} \end{aligned}$$

For maximum *prolate alignment* all spins are pointing along the Z-axis ( $A > 0$ ), and maximum alignment  $A = +1$  is obtained if  $\alpha_2(\max)$  is:

$$|\alpha_2(m=I)| = I(2I-1) \quad \text{for any spin.}$$

The alignment is then related to the second order orientation tensor as follows:

$$B_2^0 = \frac{\sqrt{5}|\alpha_2(\max)|}{\sqrt{I(I+1)(2I+3)(2I-1)}} A. \quad (4)$$

Remark that in general an aligned ensemble is described by the orientation tensors of even rank  $k$ :  $B_2^0$ ,  $B_4^0$ , etc. Odd tensor ranks are zero. For some cases one can limit to the lowest order only, and thus describe the orientation by one parameter  $A$ . This has however to be studied case by case.

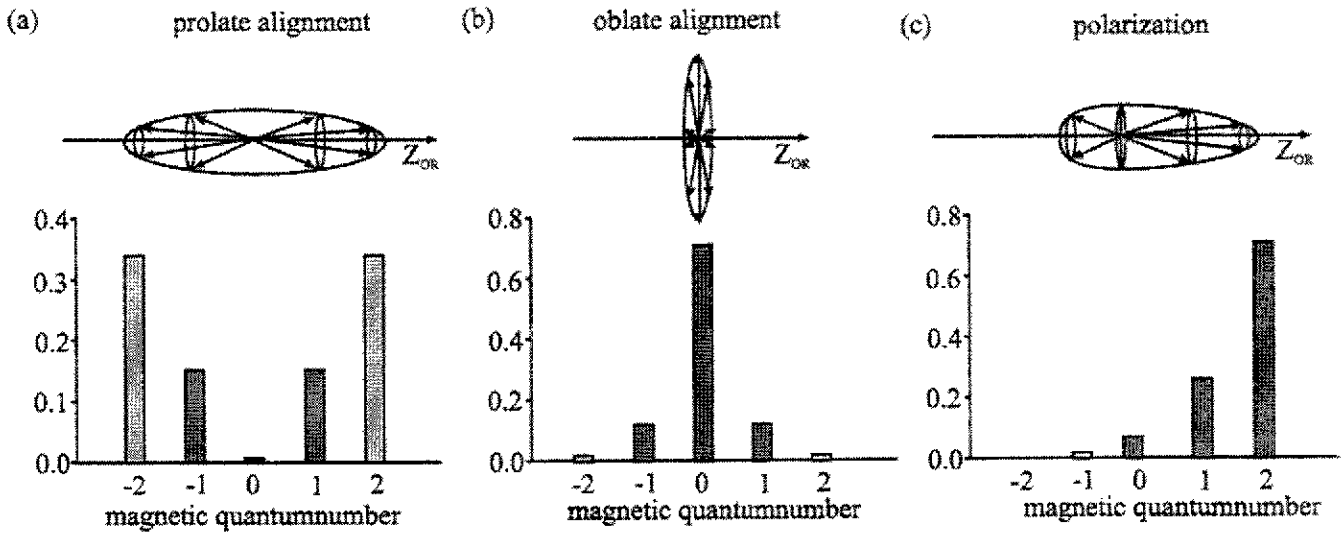


Figure 2: Examples to demonstrate different types of orientation.

### II.2.b Polarization of nuclear spins.

An ensemble of nuclei is polarized if the up/down symmetry along the axial symmetry axis is broken:

$p_m \neq p_{-m}$ . The nuclear polarization is proportional to  $\sum_m m p_m$  and is related to the orientation tensor of

first order:

$$\begin{aligned} B_1^0 &= \sqrt{2I+1}\sqrt{3} \sum_m (-1)^{I-m} \begin{pmatrix} I & I & 1 \\ -m & m & 0 \end{pmatrix} p_m \\ &= \frac{-\sqrt{3}}{\sqrt{I(I+1)}} \sum_m m p_m \end{aligned} \quad (5)$$



The normalized polarization is defined such that  $P = +1$  if all spins are parallel to the Z-axis, and  $P = -1$  for all spins are anti-parallel to the Z-axis :

$$P = \frac{\sum m p_m}{I} \quad (6)$$

and consequently the relation between the polarization and first order orientation tensor is :

$$B_1^0 = \frac{-\sqrt{3}I}{\sqrt{(I+1)}} P. \quad (7)$$

In general, a polarized ensemble is described by both even and odd tensor components. However, one will generally be able to limit to the first order term only in the angular distribution, for example if one studies the asymmetry in  $\beta$ -decay (see further).

### II.2.c. Methods to obtain oriented nuclei

We give a few examples of methods that can be used to orient nuclei, without discussing these methods in detail. Details can be found in the references. Here we mainly restrict to the region of applicability regarding lifetime, production, type of element, etc... Remark that the list is not complete, other techniques might exist.

- One of the oldest methods to polarize nuclear spins is probably the **Low Temperature Nuclear Orientation Method** <sup>13)</sup>. It was used for the first time, in the experiment of Wu et al. <sup>14)</sup> who polarized the nuclear spins of <sup>60</sup>Co to show the parity violation in  $\beta$ -decay. With this technique, nuclei are implanted into a ferromagnetic host that is cooled down to extremely low temperatures (mK). The nuclei should have lifetimes of order of seconds or higher, and therefore this technique is in general not suited to study nuclei very far from stability where lifetimes become short. Typical amounts of polarization are of the order of 10-20%.
- Using **beams of polarized electrons, deuterons, neutrons, tritons**, allows to obtain polarized radioactive nuclei, but only near to stability <sup>15)</sup>.
- A technique which has been applied successfully in a few experiments and can be applied for a wide range of nuclei produced by whatever means, is the **tilted foil polarization method** <sup>16)</sup>. It is however a difficult polarization technique, which requires a lot of

investigation case by case, and gives in general small amounts of polarization (order of few percent).

- A very efficient technique to obtain a radioactive beam of highly polarized nuclei (typically  $P \sim 30-50\%$ ) is the **Optical Pumping** method<sup>17)</sup>. This technique is based on the interaction between the electron spins and the nuclear spin, which allows to transfer electron polarization to nuclear polarization. The electrons are polarized by bombardment of the atomic beam with a circularly polarized laser beam. A long enough interaction time between the laser and atomic beam is needed to obtain full polarization by the pumping technique. Some very successful experiments using this orientation technique are described in ref. [17] and [18] and references therein.
- The easiest way to get a spin-oriented ensemble of radioactive nuclei, is if the **orientation is produced during the production reaction itself**. This is the case for isomers produced in a fusion evaporation reaction<sup>19,20)</sup>. It has been shown that for all (Heavy Ion, xn) and (alfa,xn) reactions, the spin-alignment of the isomers can be described by a Gaussian Distribution

function 
$$p_m = \frac{e^{-m^2/2\sigma^2}}{\sum_m e^{-m^2/2\sigma^2}},$$
 with a typical width  $\sigma/I = 0.3-0.4$ , corresponding to high

alignments of the order of 50% or more.

But also fragments produced in an intermediate energy projectile fragmentation reaction are shown to be spin-aligned<sup>21)</sup> (if selected in forward direction with respect to primary beam) or spin-polarized<sup>22)</sup> (if selected at a finite angle with respect to the primary beam direction). Typical values here are of the order of 10-20% of spin orientation. Using the spin-orientation obtained in projectile fragmentation, one is able to study moments of very exotic nuclei. Projects in this field are being performed at all fragmentation facilities<sup>23,24,25,26)</sup>. However, the mechanism is still not fully understood and it is not yet possible to make predictions on the optimal conditions and the amount of orientation that can be obtained.

### II.3. Perturbation of the spin-orientation by interaction with EM fields

### II.3.a Interaction with static magnetic field and RF-field : NMR

The interaction between a nucleus with spin  $I$  and a static magnetic field  $B_0$  causes a splitting of the nuclear hyperfine levels (the  $m$ -states). The Hamiltonian describing this interaction (Zeeman Interaction) is  $H_B = -\vec{\mu} \cdot \vec{B}_0$ , with  $\vec{\mu} = g\mu_N \vec{I}$  the magnetic moment. The  $|m\rangle$ -states are eigenstates of this Hamiltonian with eigenvalues  $E_m = -\hbar\omega_L m$  and  $\omega_L = \frac{g\mu_N B_0}{\hbar}$  (8)

the Larmor frequency. In figure 3 a typical Zeeman splitting is shown, with equidistant level splitting between  $m$ -states. By adding a radio frequency (RF) field  $B_1(t)$  in the plane perpendicular to the static field, the Hamiltonian is no longer axial symmetric and thus the  $|m\rangle$  states are no longer eigenstates. It can be shown <sup>27)</sup> that this breaking of the axial symmetry will cause a mixing of the  $|m\rangle$  states if the RF-frequency matches the Larmor frequency :  $\omega_L = \omega_{RF}$ . At that moment, the level populations  $p_m$  are all equalized and this change of the spin-orientation can be detected in the asymmetry of the radioactive decay. By looking for the resonance frequency  $\omega_{RF}$  at which the spin-orientation is modified, one can thus determine the nuclear  $g$ -factor. The experimental technique in which the resonant change of the asymmetry of the  $\beta$ -decay is measured as a function of the applied RF-frequency is called the **Nuclear Magnetic Resonance (NMR)** method.

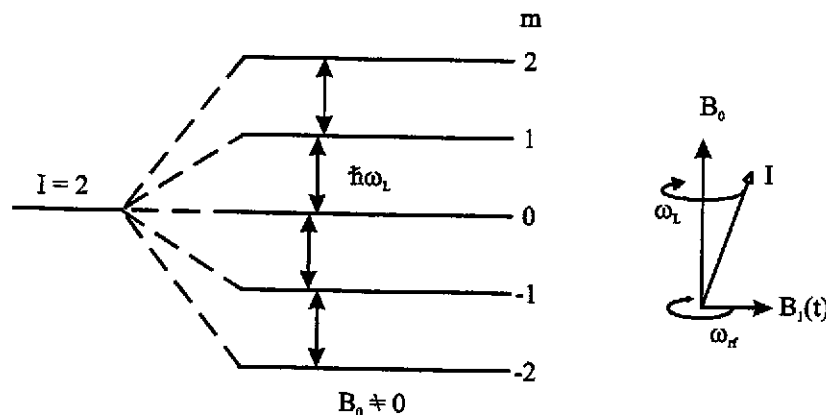


Figure 3: The quantum states  $|m\rangle$  of a nucleus with spin  $I$  in a magnetic field  $B_0$  are no longer degenerate. The energy splitting is equidistant and proportional to the nuclear  $g$ -factor. By applying an RF-field with frequency  $2\pi\nu_{RF}$  the level populations  $p_m$  are equalized when  $\nu_{RF} = \nu_L$ .

Remark that for an initially aligned ensemble of nuclei, no change in the  $\beta$ -asymmetry can be detected, because no spin-polarization is present initially, nor it is induced by the RF-interaction. This means

that in order to detect an NMR resonance, the nuclear spins need to be initially polarized before implanted in the stopper.

### II.3.a Interaction with an electric field gradient and RF-field : NOR

A nucleus that is stopped in a material that has a non-cubic lattice structure, will exhibit an interaction between the non-spherical nuclear charge distribution (reflected by a non-zero spectroscopic quadrupole moment  $Q$ ) and the electric field gradient induced by the lattice on the implanted nucleus. For an axial symmetric electric field gradient, the Hamiltonian of the quadrupole interaction is described easiest in a reference frame fixed to the principle axis system of the axial symmetric electric

$$\text{field } V_{zz} \text{ }^{28)}: H_Q = \frac{\omega_Q}{\hbar} (3I_z^2 - I^2), \text{ with } \omega_Q = \frac{eQV_{zz}}{4I(2I-1)\hbar} \quad (9)$$

the quadrupole interaction frequency. Another definition sometimes used for the quadrupole frequency

$$\text{is } \nu_Q = \frac{eQV_{zz}}{h} = \frac{\omega_Q 4I(2I-1)}{2\pi}. \quad (10)$$

The projection of the spin-operator onto the Z-axis of the principle axis system ( $|m\rangle$ -state) is an eigenstate of this Hamiltonian with eigenvalue  $E_m = \hbar\omega_Q[3m^2 - I(I+1)]$ . In figure 4 a typical quadrupole splitting is shown, with non-equidistant level splitting between  $m$ -states, and degeneracy of  $-m$  and  $+m$  levels.

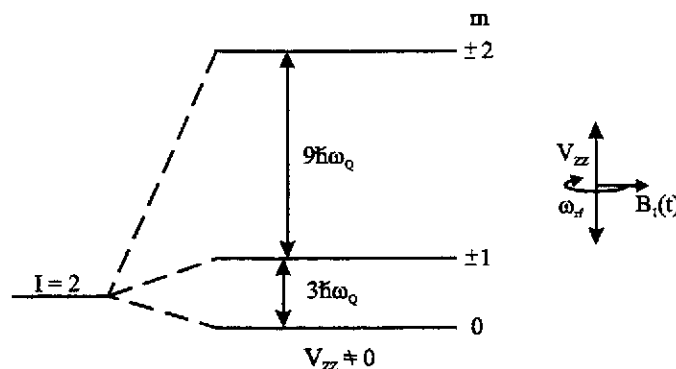


*Figure 4 : Non-equidistant level splitting of a nucleus submitted to a quadrupole interaction. Consequently different RF-frequencies can give rise to a quadrupole resonance in the asymmetry of a  $\beta$ -decaying nucleus. The resonance frequencies contain information on the quadrupole frequency.*

By adding an (RF) field  $B_1(t)$  in the plane perpendicular to the symmetry axis of the EFG, the Hamiltonian is no longer axial symmetric and thus the  $|m\rangle$  states are no longer eigenstates. Again this breaking of the axial symmetry will cause a mixing of the  $|m\rangle$  states, in this case if the RF-frequency

matches one of the quadrupole splitting frequencies:  $\Delta\omega_Q = 3(2m-1)\omega_Q = \omega_{RF}$ . At that moment, the level populations of two levels  $p_m$  and  $p_{m+1}$  are equalized and this change of the spin-orientation can be detected in the asymmetry of the radioactive decay. However, if the populations probabilities of the  $|m\rangle$  and  $|m+1\rangle$  levels are equalized by the RF, also the  $p_m$  and  $p_{-m}$  are equalized because the  $\pm m$  levels are degenerate. Thus a change in the polarization ( $p_m \neq p_{-m}$ ) can only be detected if the spins are polarized before the RF-interaction takes place. A destruction of the initial polarization can then induced by the RF-interaction which will mix the population of levels with  $\Delta m=1$ . By looking for the resonance frequencies  $\omega_{RF}$  at which the spin-orientation is modified, one can thus determine the quadrupole interaction frequency. If the electric field gradient can be determined by some other technique, the nuclear quadrupole moment is deduced. The experimental technique in which the asymmetry of the  $\beta$ -decay is changed due to a quadrupole interaction, and in which this change is measured as a function of the applied RF-frequency is called the **Nuclear Quadrupole Resonance (NQR)** method. Over the years, several highly sophisticated versions of this technique have been developed, such as a multiple frequency NQR<sup>29,30</sup>.

The spectroscopic quadrupole moment of a nuclear state can only be measured for states with spin  $I \geq 1$ . This follows immediately from the definition of the quadrupole moment<sup>31</sup>, which is the expectation value of the  $M_2$ -operator for  $m=I$ :  $Q \equiv \langle I m | M_2^0 | I m \rangle_{m=I}$ . Using the Wigner-Eckart theorem, one can express  $Q$  as a function of the reduced matrix element and a 3J symbol  $\begin{pmatrix} I & 2 & I \\ -m & 0 & m \end{pmatrix}$ . For a nucleus with  $I=1/2$  the 3J symbol for an operator of order two is zero, and thus  $Q=0$ . This does not mean that such a nuclear state can not be deformed, but simply that it can not be measured by measuring the static quadrupole moment.

#### II.4. Measure the change of the spin-orientation: angular distribution of the radiation

The emission of radiation from a radioactive nuclear state is related to the direction of its spin. The relation which expresses the angular distribution of radiation emitted in a particular direction  $(\theta, \varphi)$  with respect to a chosen axis system is given by:

$$W(\theta, \varphi, t) = \sum_{k,n} \frac{\sqrt{4\pi}}{\sqrt{2k+1}} A_k(\gamma, \beta, \dots) B_k^n(I, \omega_L, \omega_Q, t) Y_k^n(\theta, \varphi). \quad (11)$$

$A_k$  are the radiation parameters describing the type of radiation and its properties (for example M1, E2, ...).  $B_k$  are the orientation tensors of order  $k$ : they describe the orientation of the ensemble spin, and its change due to interaction with the surrounding fields. It is this parameter that needs to be calculated to describe the influence of a particular interaction on the spin orientation. We will see further how this can be done.  $Y_k$  are the spherical harmonics: they depend on the position of the detectors with respect to the chosen axis system (the same as in which the interaction with the fields is described).

The angular distribution function can be simplified for particular types of radiation. If  $\gamma$ -radiation is detected, only radiation parameters with  $k$ =even are non-zero and the angular distribution is reduced to even order tensor components. Consequently only alignment ( $B_2, B_4, \dots$ ) can be measured by  $\gamma$ -radiation.

If the nucleus is decaying by  $\beta$ -decay, one can generally reduce the angular distribution function to the first order tensor (for allowed beta decay only  $A_1 \neq 0$ ), which means that  $\beta$ -decay is mainly sensitive to nuclear polarization. Furthermore, if one puts the detectors at  $0^\circ$  and  $180^\circ$  with respect to the Z-axis of the chosen system (for example parallel to a static field), then only  $n=0$  tensor components are non-zero and thus the angular distribution function for  $\beta$ -decay simplifies to:

$$W(\theta, \varphi, t) = 1 + A_1 B_1(I, \omega_L, \omega_Q, t) \cos \theta \quad (12)$$

The orientation tensor of a system perturbed by some interactions, can be described as a function of the perturbation factors and the initial orientation tensor as follows:

$$B_1^0(I, \omega_L, \omega_Q, t) = \sum_{k,n} G_{1k}^{0n}(I, \omega_L, \omega_Q, t) B_k^n(I, t=0) \quad (13)$$

This expression shows that in order to be able to measure an odd tensor orientation (polarization), one needs to have initial polarization unless an interaction is applied which allows transforming alignment

into polarization (thus  $G_{12}^{0n}(I, \omega_B, \omega_Q, t) \neq 0$ ). We will see in chapter IV that this requires some special features of the applied interactions and the formalism which allows to calculate the perturbation factor will be explained by applying it for a particular case.

### III. SOME EXAMPLES OF EXPERIMENTAL TECHNIQUES

#### III.1. As a function of time: TDPAD

The **Time Differential Perturbed Angular Distribution** method has been used for many years to study the magnetic dipole or the electric quadrupole moments of isomers produced in fusion-evaporation reactions<sup>1,32</sup>. Also a few isomers populated and spin-oriented by coulomb excitation, and having a suitable lifetime ( $50\text{ns} < \tau < 10 \mu\text{s}$ ), have been used as probes to study the quadrupole interaction in materials<sup>33,34</sup>. Recently it has been applied also on isomers produced in projectile fragmentation, after they are selected using a high-resolution in-flight recoil spectrometer (like LISE at GANIL)<sup>35,36</sup>.

To study the magnetic moment, the isomers are produced or recoil-implanted into a stopper with a cubic lattice structure (polycrystalline foil or single crystal). A static magnetic field is applied perpendicular to the symmetry axis of the initial spin orientation. This orientation axis is in the horizontal plane: parallel to the primary beam direction if the isomers are implanted directly after the reaction, or rotated over an angle  $\gamma$  for mass-separated isomers<sup>37</sup>. It means the magnetic field is applied vertically (we choose Z-axis along this direction, fig. 5).

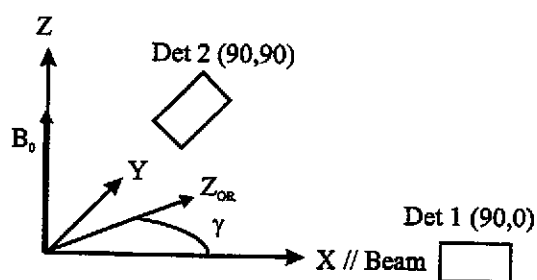


Figure 5 : Definition of different axis systems involved in the formal description of the interactions and orientation involved in a TDPAD experiment:  $(X, Y, Z)$  is the system fixed to the magnetic field and in which the detector positions are described (LAB-system). The  $(X, Y, Z)_{OR}$  system has its Z-axis along the axial symmetry axis of the initial orientation, allowing an easy description of the orientation.

The nuclear spins will perform a Larmor precession around the static field. This precession can be detected by putting detectors in the horizontal plane. If the spin ensemble is initially spin-aligned, for example along the  $Z_{or}$  direction as defined in figure 5, the change of the spin-orientation can be registered as a function of time. The angular distribution for an aligned ensemble interacting with a static field, and decaying by gamma-radiation with a lifetime  $\tau$ , is given by <sup>38)</sup>:

$$W(\theta, \varphi, t) = e^{-t/\tau} (1 + A_2 \sum_n B_2^n(I, \omega_L, t) Y_2^n(\theta, \varphi) \sqrt{\frac{4\pi}{5}} + \dots) \quad (14)$$

in which  $B_2^n$  describes the perturbation of the initially aligned ensemble. One can show that for the set-up as given in fig. 5, this perturbed orientation tensor has only a second order component that depends on time, while the zero-order component is proportional to the initial orientation:

$$B_2^n(t) = e^{-in\omega_L t} B_2^n(t=0)_{LAB}. \quad (15)$$

Taking into account that the initial orientation is parallel to  $Z_{or}$  (and thus described by one tensor component  $B_2^0(t=0)_{OR}$ ), and transforming all tensors to the LAB-frame using the Wigner rotation matrices <sup>12)</sup>, we find for the angular distribution:

$$W(\varphi, t) = e^{-t/\tau} \left( 1 + B_2^0(t=0)_{OR} \left[ \frac{1}{4} A_2 + \frac{3}{4} A_2 \cos(2\omega_L t + 2\gamma - 2\varphi) \right] \right) \quad (16)$$

For two detectors placed respectively at angles  $\varphi_1$  and  $\varphi_2$ , the  $R(t)$  function is defined such that it simply depends on the cosine function, which describes the pure Larmor precession:

$$\begin{aligned} R(t) &= \frac{N(\varphi_1) - \varepsilon N(\varphi_2)}{N(\varphi_1) + \varepsilon N(\varphi_2)} \\ &= \frac{3}{4} A_2 B_2^0(t=0) \sin(\Delta\varphi) \sin(2\omega_L t + 2\gamma - (\varphi_1 + \varphi_2)) \end{aligned} \quad (17)$$

Remark that for two detectors placed a  $\Delta\varphi=90^\circ$ , the maximum amplitude of the wiggles can be detected. This is thus the optimal setting for a TDPAD experiment.

A similar expression can be derived in the case that the host induces an electric field gradient at the position of the implanted isomer. In that case a superposition of cosine functions occurs with frequencies that are multiples of the basic quadrupole frequency  $3\omega_Q$ .



### III.2. As a function of an applied RF-frequency: NMR, NQR

The Nuclear Magnetic Resonance and Nuclear Quadrupole Resonance techniques are *time integrated* perturbation angular distribution techniques. If the angular distribution described previously is averaged over the decay time (so a time-integrated experiment is performed), most information on the angular distribution is lost. In a time integrated experiment one needs to apply an extra perturbing interaction, in order to induce a change of the spin-orientation.

Such an interaction is for example a radio frequency (RF) magnetic field that is placed perpendicular to the static field direction (fig. 6). In an NMR experiment the nuclei of interest are implanted into a cubic crystal; in an NQR experiment a host with an electric field gradient is needed. These techniques have been applied only to ground states (lifetimes between 1 ms and 10 sec) till now, mainly because the radioactive nuclear state needs to live sufficiently long in order to be sensitive to the RF-perturbation. As ground states mostly decay by  $\beta$ -decay, it means these experiments are measuring the polarization change in the spin orientation. Therefore a static magnetic field is applied parallel to the direction of the initial spin-polarization. The polarization is then modified during the lifetime of the nucleus, when implanted into a stopper, by applying an RF-field  $B_1(t)$  perpendicular to the static field. This experimental technique has been widely described in literature, for example in ref. 15,18,23, 29,39,40.

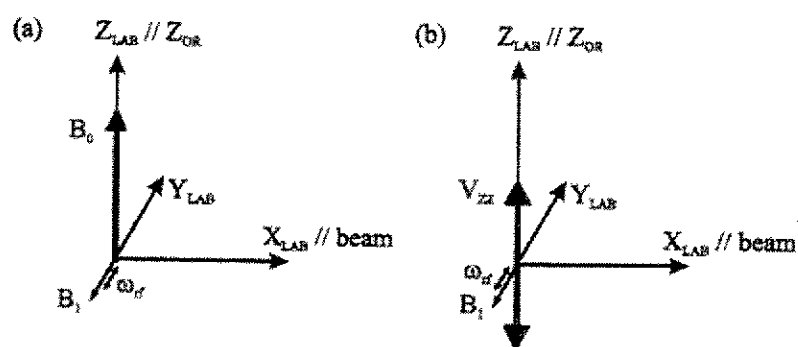


Figure 6: Symmetry axes of the interactions and the spin-orientation for NMR (a) or NQR (b) experiment.

### III.3. As a function of the static field $B_z$ : LMR and LEMS

Another type of time integrated PAD experiments are based on the nuclear "Level Mixing" principle. In the next chapter we will discuss this method more in detail. Here we briefly give an overview of the history of the technique.

It has been well known *in atoms* that crossing and anti-crossing of atomic levels can occur if atoms are submitted to a combination of static electric and magnetic fields <sup>41)</sup>. A similar type of crossing of *nuclear hyperfine levels* has been described theoretically in the sixties <sup>42)</sup>. Matthias showed that the  $m$ -quantum states of nuclei with spin  $I$ , that are submitted to a combined magnetic field and electric field gradient, are crossing as a function of the applied magnetic field strength if the magnetic field is placed parallel to the symmetry axis of the electric field gradient (fig. 7a). If a small misalignment angle  $\beta$  is introduced between the two interaction axes, anti-crossing of the levels occurs (fig. 7b).

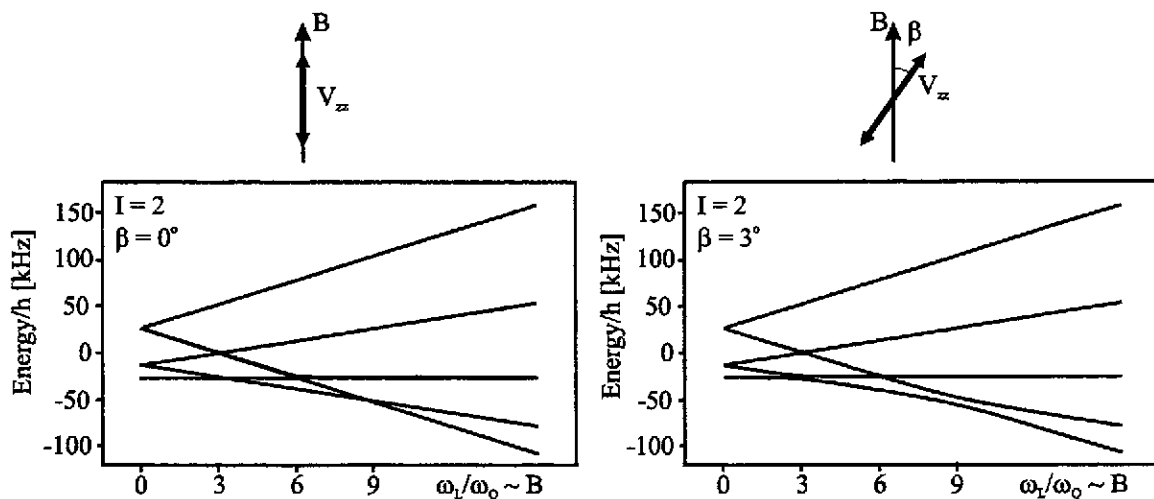


Figure 7: (a) When nuclei are submitted to a collinear magnetic field and electric field gradient, the  $m$ -quantum states are crossing at well-defined values of the magnetic to quadrupole interaction frequency. (b) If the two interactions are not collinear, the degeneracy of the crossing levels does no longer occur and the levels are anti-crossing (= mixing).

About a decade later, it was shown experimentally that crossing or anti-crossing of nuclear hyperfine levels gives rise to a resonant change in the angular distribution of radioactive decay of ground states <sup>43)</sup> or isomeric states <sup>44)</sup>. A full description of the theoretical formalism which allows to describe and understand the features of these resonances in the angular distribution was developed by the group of

Coussement in the eighties<sup>45,46,47</sup>. This group has been investigating all features of the “Level Mixing” resonances both theoretically and experimentally<sup>48,49</sup>. In figures 8 and 9 some simulations of the angular distribution of radioactive decay as a function of the applied magnetic field strength are given for nuclei submitted to a level mixing interaction. The origin of the term “Level Mixing” becomes clear when the level populations of the m-states are calculated in a two-level approximation using the density matrix formalism<sup>47</sup> (section IV). Then it appears clearly that the non-collinearity of the magnetic and electric interactions are causing a local “mixing” of the level populations.

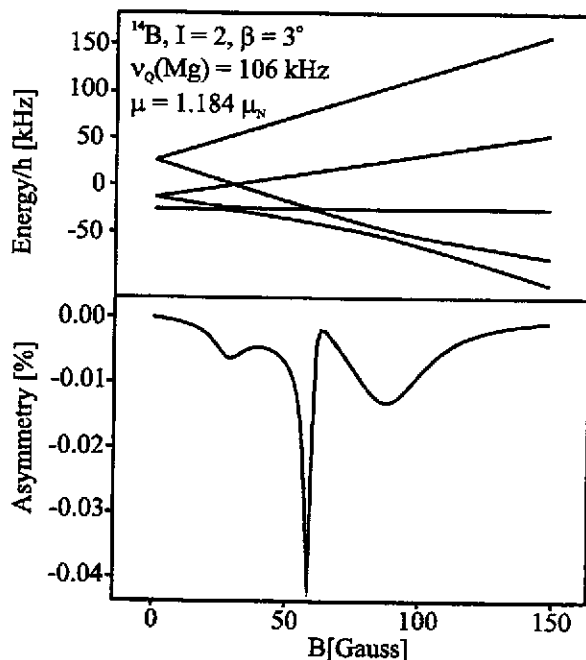


Figure 8: Simulation of an LMR-curve for  $^{14}\text{B}$ -fragments produced at the LISE3 spectrometer in GANIL. The resonances due to different level mixings are visible in the asymmetry of the beta-decay of spin-aligned projectile fragments. Remark that spin-polarization (and thus  $\beta$ -asymmetry) is induced in the resonances and that the polarization is zero out of the resonance region.

Although the resonances were originally investigated mainly as a curiosity, it became clear that the **Level Mixing Resonance (LMR)** technique could be very useful as a tool to study the quadrupole moment of nuclear ground states and isomeric states. Several variations of the Level Mixing technique were developed.

A first useful application of the level mixing formalism was to study the quadrupole moments of high-spin isomers (using the **Level Mixing Spectroscopy, LEMS-method**)<sup>50,51,52,53</sup>. This method has some clear advantages with respect to the classical TDPAD method (as described in next section).

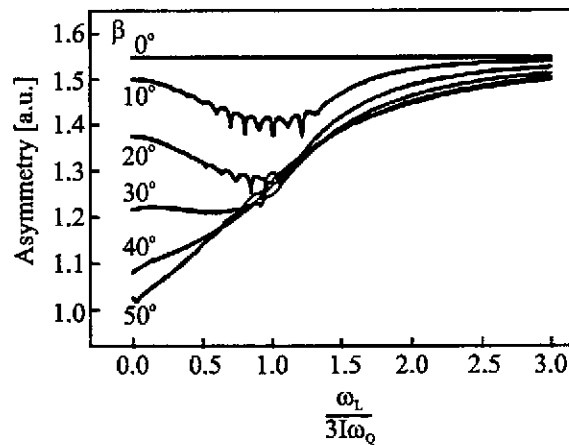


Figure 9 : Simulation of LMR-curves for a high-spin state ( $I=10$ ) and for different misalignment angles between the magnetic and electric interaction. At small angles many resonances are appearing with relatively small amplitudes and thus hard to measure experimentally. However for large angles  $\beta$  a decoupling curve is appearing. This decoupling curve is also sensitive to the ratio of the magnetic to quadrupole moment of a high-spin isomer. To distinguish the decoupling curves from the LMR-curves, they are called LEMS-curves (LEvel Mixing Spectroscopy).

Another interesting use of the level mixing formalism is to study nuclear moments of exotic nuclei produced and spin-aligned in a projectile fragmentation reaction<sup>25,54,55</sup>. The strength of the  $\beta$ -LMR method is that it is possible to induce spin-polarization in an ensemble of initially spin-aligned nuclei. This has the great advantage that exotic nuclei produced in projectile fragmentation and selected in the forward direction (and thus with the highest yield) can be used to investigate their nuclear moments<sup>56</sup>. For the classical NMR technique, an initially polarized ensemble is needed to allow a beta-asymmetry measurement. And polarization is obtained only if fragments are selected at a finite angle with respect to the primary beam (and thus with a lower yield in intermediate and high-energy reactions).

### III.4. Comparison and applicability of the presented techniques.

In table 1 we present schematically the regions of applicability, for example concerning spin, lifetime and type of the nuclear states that can be investigated by a particular method. We also compare the parameters that are deduced and the accuracy that can be reached.

With the TDPAD method one can measure either the magnetic or the quadrupole moment of isomeric states in nuclei, depending on the crystallographic nature of the host (cubic lattice or a non-cubic structure inducing an EFG). The same holds for the NMR and NQR methods, allowing to measure respectively  $\mu$  or  $Q$  of nuclear ground states. With the LMR method one measures the ratio of the nuclear moments  $\mu/Q$  both for ground states ( $\beta$ -LMR) and isomeric states ( $\gamma$ -LMR), and thus  $Q$  can be deduced if  $\mu$  was measured by another method. A combination of the LMR and NMR techniques in one experiment allows the determination of both ground state moments independently<sup>55,56</sup>. Each of these methods allows measuring the nuclear moments with very high accuracy (order of 1% or better) because it are resonant techniques. The LEMS method on the other hand is a decoupling technique and is consequently less sensitive to measure the nuclear moment ratio (typically 10-15%).

However, the LEMS technique is the only method that allows measuring the static quadrupole moment of long-lived ( $\tau > 10 \mu\text{s}$ ) high-spin isomers. The TDPAD method is less suitable to study the quadrupole moment of very high-spin states because the number of quadrupole frequencies increases with spin. The method is not at all applicable to study long-lived isomers, because it is a time differential technique.

*Table 1: Comparison of the presented techniques to measure nuclear moments.*

	<b>TDPAD</b>	<b>NMR/NQR</b>	<b>LMR/LEMS</b>
Type of nuclear state	Isomer	Groundstate	Both
Spin	$0.5 - 20 \hbar$	$0.5 - \dots \hbar / 1 - 3 \hbar$	$1-5 \hbar / 1 - \dots \hbar$
Lifetime range	10 ns – 10 $\mu\text{s}$	1 ms – 1 s	1 ms – 1 s / 50 ns – 1 s
Initial Spin-orientation	Alignment	Polarization	both
Detected radiation	$\gamma$	$\beta$	both
Deduced parameter	$g, Q$	$g, Q$	$Q/\mu$
Accuracy	< 5%	< 5%	<5% / < 20%

The upper limit on the lifetime of the isomers that can be studied by a time differential technique, is determined by two causes: the duty-cycle of the accelerator (and thus production efficiency) and the spin-spin relaxation time<sup>57)</sup>. For a time differential experiment, one needs a pulsed beam with a short production pulse and a long (about 3 lifetimes) measuring time. This puts automatically an upper limit on the lifetime: for too long-lived isomers the production efficiency drops drastically making the measurement very inefficient or even impossible. On the other hand, the spin-spin relaxation mechanism also prevents experiments on long-lived isomers because it causes a damping of the oscillation pattern as a function of time. Relaxation times depend strongly on the stopper material that is used. Typical values for the spin-spin relaxation (damping) time are of the order of microseconds. Time integrated methods are limited by the much longer spin-lattice relaxation time<sup>58,59)</sup>: the interaction between the nuclear spin and the electron spin of free electrons in metal hosts will cause a loss of the spin-orientation. If the spin-lattice interaction time is shorter than the isomeric lifetime, the information regarding the static interactions is lost. Spin-lattice relaxation times also depend strongly on the host material as well as on the type of probe that is studied. It is well known that for metallic hosts the relaxation time can be increased by decreasing the host temperature<sup>59)</sup>. The relaxation times can vary from a few 100  $\mu\text{s}$  up to several seconds.

The lower limit on the lifetime of isomers that can be studied by the TDPAD technique is typically of the order of 10 ns up to 10  $\mu\text{s}$ . For all hyperfine interaction techniques, this lower limit is determined by the uncertainty relation  $\omega_p \tau > 1$ : the perturbing magnetic or quadrupole interaction needs to be strong enough (fast enough frequency  $\omega_p$ ) in order to see the perturbation in the spin-orientation during the lifetime  $\tau$  of the isomer. For typical magnetic fields of the order of a Tesla, or electric field gradients of the order of  $10^{17}$  V/cm<sup>2</sup>, this results in a lower lifetime limit of the order of tens of nanoseconds for the time differential technique. For time integrated techniques like the NMR, NQR, LMR, LEMS methods, the lower limit is about 3-5 times higher, because the time integration over an oscillating function results in a full destruction of the initial spin-orientation (and thus full effect in the measured anisotropy change) only if averages over several oscillation periods are taken.

#### IV. THE LEVEL MIXING FORMALISM:

##### FROM QUANTUM MECHANICAL CURIOSITY TO A NUCLEAR PHYSICS METHOD

#### IV.1. The combined interaction system and the density matrix approach.

In this chapter we will explain how the perturbed angular distribution of nuclear radiation can be calculated starting from the Hamiltonian that describes the interaction of the nuclear spins with the electromagnetic fields in their surroundings. The nuclei can be produced by several reactions, and need to be spin-oriented before implantation in a suitable stopper. For each type of production reaction, spin-orientation mechanism and perturbing interaction, a different formalism has to be developed.

To illustrate how we can calculate the perturbation of an initially oriented ensemble of nuclei by the interaction of the nuclei with some fields, we will chose the particular example of Level Mixing Resonances induced by a combined magnetic dipole and electric quadrupole interaction. The electric interaction occurs by implanting the probe nuclei into a lattice with a non-cubic symmetry<sup>42)</sup> inducing an electric field gradient on the position of the probe nuclei. The magnetic interaction is provided by putting the host material into a static magnetic field  $\mathbf{B}$ . The Hamiltonian of this combined interaction system is given by<sup>42,45)</sup>:

$$\begin{aligned}
 H &= H_Q + H_B \\
 &= \frac{4\pi}{5} \sum_q (-)^q T_q^2 V_{-q}^2 - \boldsymbol{\mu} \cdot \mathbf{B}
 \end{aligned}
 \tag{18}$$

with  $T^2$  the electric quadrupole tensor,  $V^2$  the electric field gradient tensor and  $\boldsymbol{\mu}$  the magnetic dipole vector. To give an explicit expression for the quadrupole interaction Hamiltonian  $H_Q$  one needs to specify the axis system in which the interaction will be described. In the PAS system the electric field gradient is fully described by two parameters: the field gradient strength along the  $Z_{\text{pas}}$  axis ( $V_{zz}$ ) and the asymmetry parameter  $\eta$ . For an axially symmetric electric field gradient ( $\eta=0$ ), the Hamiltonian is given by expression (9) if expressed in the PAS system.

If also a magnetic field is present, one can define a second axis system in which the magnetic field is parallel to the Z-axis (LAB-system). If one wants to express  $H_Q$  in the LAB frame, an Euler rotation

from PAS to LAB over the angles  $(0, -\beta, -\alpha)$  needs to be performed (figure 10)<sup>12)</sup>. The Hamiltonian of the quadrupole interaction expressed in the LAB-system is discussed in reference 42.

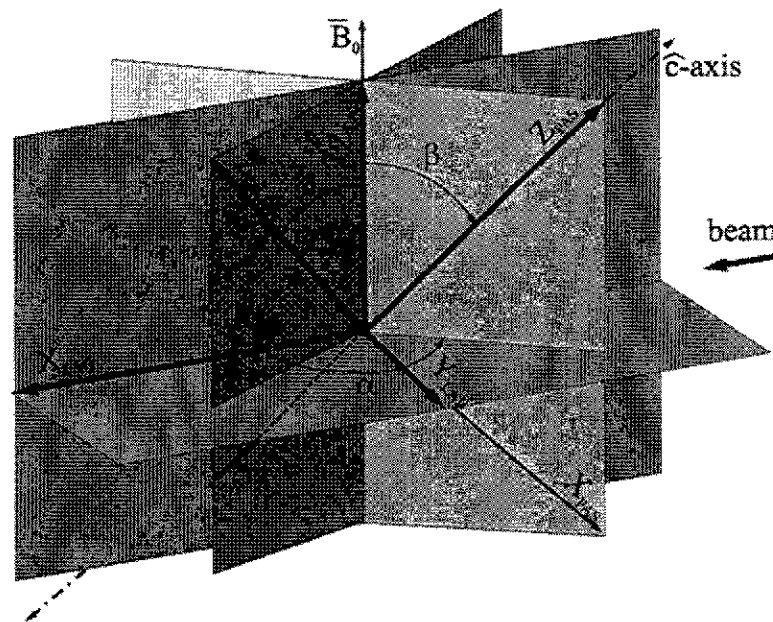


Figure 10 : Definition of the Euler angles between the Principle Axis System (PAS) connected to the electric field gradient and the LAB(oratory) system connected to the magnetic field. In the picture also the Euler angles to rotate from the LAB-frame to a system with the  $Z_{lab}$  axis parallel to the axial symmetry axis of the initial orientation are defined.

For an axially symmetric electric field gradient, one can define the rotation from the PAS-system to the LAB system by one angle  $\beta$  because  $\alpha$  can be chosen zero. The combined interaction Hamiltonian can be written in the PAS by projection of  $B$  into the  $(X_{pas}, Z_{pas})$  frame, and consists of an axially symmetric part ( $\sim I_{Z_{pas}}$ ) and a symmetry breaking part ( $\sim I_{X_{pas}}$ ):

$$\begin{aligned}
 H &= H_{\parallel} + H_{\perp} \\
 &= \frac{\omega_Q}{\hbar} (3I_{Z_{pas}}^2 - I^2) - \omega_L \cos \beta I_{Z_{pas}} + \omega_L \sin \beta I_{X_{pas}}
 \end{aligned}
 \tag{19}$$

The eigenstates of this Hamiltonian are no longer the eigenstates  $|lm\rangle$  of the spin operator, because of the ladder operators in the symmetry breaking term ( $H_{\perp} \sim I_{\pm} \sim (\Gamma + I)$ ). To find the  $(2I+1)$  eigenstates  $|N\rangle$  of this Hamiltonian, we can apply a numerical diagonalisation procedure. This is what we do if we perform a numerical simulation for the eigenvalues (Rabi plot) and the angular distribution (LMR or LEMS curves) as a function of  $B$ .



However, an analytical calculation gives us a much better insight into the nature of the eigenstates. To obtain that, we will calculate the eigenstates in a first approximation using first order quasi-degenerate perturbation theory<sup>60</sup>. This is possible if the misalignment angle  $\beta$  is small enough: in that case the symmetry breaking term modifies the axial symmetric eigenvalues only if they are quasi-degenerate. The eigenvalues of the axial symmetric part  $H_{\parallel}$  are given by:

$$E_m = \hbar\omega_Q [3m^2 - I(I+1)] - \hbar\omega_L \cos \beta \quad (20)$$

and degeneracies (level-crossing) occur if  $\omega_L \cos \beta = 3\omega_Q (m_1 + m_2)$ . (21)

A figure where the eigenvalues are plotted as a function of  $\omega_L$  (or as a function of B) is called a Rabi plot. Examples of Rabi-plots are given in figures 7a and 7b. We see that if the angle  $\beta$  is small, the modification of the eigenvalues occurs only near these level-crossing points. This allows us to apply a **two-level approximation**: we can calculate the eigenstates of the full Hamiltonian using a quasi-degenerate perturbation theory on two quasi-degenerate levels  $E_m$  and  $E_{m'}$ . In reference 42 is described how the mixed eigenstates

$$\begin{aligned} |N\rangle &= \frac{1}{\sqrt{1+R^2}} (R|m\rangle + |m'\rangle) \\ |N'\rangle &= \frac{1}{\sqrt{1+R^2}} (|m\rangle - R|m'\rangle) \end{aligned} \quad (22)$$

with their respective eigenvalues

$$E_{N,N'} = \frac{E_m + E_{m'}}{2} \pm \frac{1}{2} \sqrt{(E_m - E_{m'})^2 + 4W_{mm'}^2} \quad (23)$$

are calculated by diagonalizing a 2x2 matrix. R is the mixing parameter defined as:

$$R = \frac{E_m - E_{m'}}{2W_{mm'}} + \frac{\sqrt{(E_m - E_{m'})^2 + 4W_{mm'}^2}}{2W_{mm'}} \quad (23a)$$

In figure 11 the unperturbed levels  $E_{m,m'}$  and the mixed levels  $E_{N,N'}$  are shown. Remark that the amount of repelling (anti-crossing) between the mixed levels is depending on the perturbation strength  $H_{\perp}$  and thus on  $\sin\beta$ :  $W_{mm'} = \langle m|H_{\perp}|m'\rangle \sim \sin\beta$ . This will also determine the width ( $\Gamma$ ) of the mixing region as a function of the field, and thus the width of the related Level Mixing Resonance in the angular distribution (see further). That means we can choose ourselves the mixing strength (and thus the resonance width) by choosing a particular angle  $\beta$  between the c-axis of the crystal and the magnetic field direction.

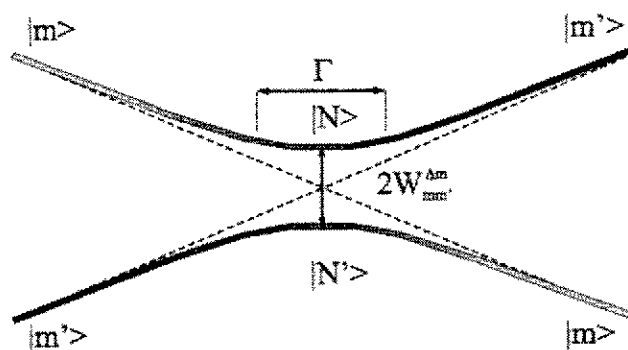


Figure 11: In a two-level approximation the eigenstates of the level mixing Hamiltonian can be calculated using perturbation theory. Near the crossing region of the unperturbed levels ( $E_m$  eigenvalues of  $H_0$ ) the symmetry breaking part of the interaction ( $H_1$ ) is mixing the states: the eigenstates of  $H$  are linear combinations of the unperturbed states. The respective energies are repelling each other.

To calculate the perturbation of the ensemble orientation one has to solve the time evolution equation of the nuclear density matrix:

$$i\hbar \frac{\partial \rho}{\partial t} = [H, \rho] \quad (24)$$

with  $H$  the level mixing Hamiltonian (18). To solve this equation, one needs to find first the eigenstates  $|N\rangle$  and eigenvalues  $E_N$  of the interaction Hamiltonian. If the Hamiltonian is expressed in the LAB-frame<sup>42</sup> the eigenstates are found by numerical diagonalisation. In that case one gets the eigenstates  $\langle N|m\rangle$  with respect to the LAB-system and they can be introduced in the perturbation factors to calculate numerically the angular distribution function (see next paragraph).

In this section we will use the analytical expression (22) of the mixed eigenstates (using the two-level approximation) with the Hamiltonian expressed in the PAS. This will allow us to get an explicit expression for the time-dependence of the density matrix and thus to understand better the nature of the resonances. For a static interaction, such as the level mixing interaction, the solution of the Von Neumann equation is given by

$$\langle N|\rho(t)|N'\rangle = \rho_{NN'}(t) = e^{-i\omega_{NN'}t} \rho_{NN'}(0) \quad (25)$$

with  $\omega_{NN'} = (E_N - E_{N'})/\hbar$  and  $E_{NN'}$  given by (23). As the LMR-method is a time-integrated measuring technique, we need to calculate the time averaged density matrix taking into account the nuclear decay time:

$$\rho_{NN'}(\tau) = \frac{\int_0^{\infty} dt \rho_{NN'}(t) e^{-t/\tau}}{\int_0^{\infty} dt e^{-t/\tau}} = \rho_{NN'}(0) \frac{1 - i\omega_{NN'}\tau}{1 + (\omega_{NN'}\tau)^2} \quad (26)$$

It is more convenient to express the density matrix in the m-representation. Using the orthogonality relation, the time integrated density matrix in the m-representation is:

$$\begin{aligned} \rho_{mm'}(\tau) &= \sum_{NN'} \rho_{NN'}(\tau) \langle m|N\rangle \rho_{NN'}(\tau) \langle N'|m'\rangle \\ &= \sum_{NN'} \langle m|N\rangle \langle N'|m'\rangle \frac{1 - i\omega_{NN'}\tau}{1 + (\omega_{NN'}\tau)^2} \rho_{NN'}(0) \end{aligned} \quad (27)$$

The density matrix of the initial orientation tensor  $\rho(0)$  is not known in the  $|N\rangle$ -basis, but can also be expressed in the m-representation:

$$\rho_{mm'}(\tau) = \sum_{NN'} \langle m|N\rangle \langle N'|m'\rangle \frac{1 - i\omega_{NN'}\tau}{1 + (\omega_{NN'}\tau)^2} \sum_{\mu\mu'} \langle N|\mu\rangle \langle \mu'|N'\rangle \rho_{\mu\mu'}(0) \quad (28)$$

If the Hamiltonian is expressed in the m-representation and if the Z-axis of this LAB-frame is parallel to the  $Z_{or}$  axis of the initial orientation, then expression (28) can be simplified because only  $\mu=\mu'$  components of the initial density matrix are non-zero.

Using the explicit expression for the eigenstates (22), eigenvalues (23) and R (23a), we can calculate the time-averaged components of the density matrix of nuclei submitted to the level mixing interaction.

The diagonal matrix elements are:

$$\rho_{mm}(\tau) = \rho_{mm}(0) + \frac{1}{2} \{ \rho_{m'm}(0) - \rho_{mm}(0) \} L_{mm'}(\tau) \quad (29)$$

and a similar expression is found for  $\rho_{m'm}(\tau)$  (by exchanging m and m').  $L_{mm'}$  is a Lorentz absorption resonance as a function of the unperturbed energy splitting:

$$L_{mm'} = \frac{(2W_{mm'})^2}{(E_m - E_{m'})^2 + (2W_{mm'})^2 + (\hbar/\tau)^2} \quad (30)$$

The time-averaged perturbed population probability  $\rho_{mm}(\tau)$  depends on the initial level population and on the population difference between the two mixing levels m and m'. For nuclei with a long lifetime  $\tau$  (larger than the perturbation  $2W_{mm'}$ ) the Lorentz function is 0 in the extremes, and becomes 1 in the

center. So if the Level Mixing condition  $2W_{mm} \gg \hbar/\tau$  is fulfilled, the amplitude of the LMR is independent of the nuclear lifetime and reaches a maximum (figure 12).

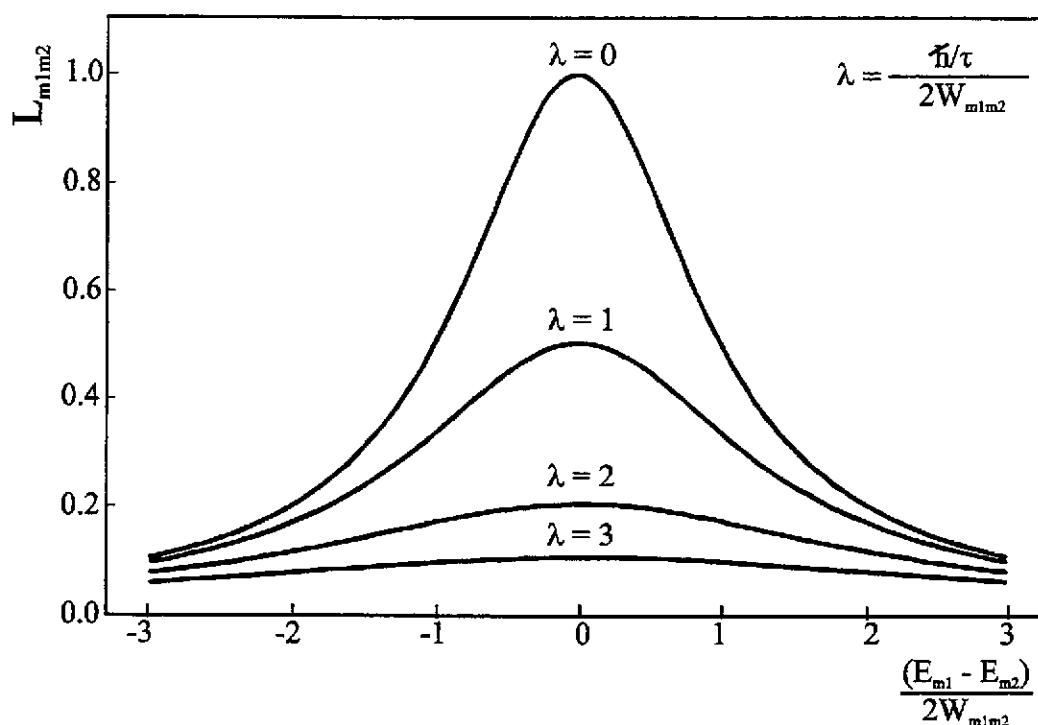


Figure 12: Simulation of the Lorentz absorption resonance as a function of the energy splitting, for nuclei with different lifetimes. Only if the lifetime is significantly longer than the inverse perturbation strength, the full amplitude of the resonance curve is obtained.

For nuclei having a sufficiently long lifetime, the two time-averaged level populations are equalized (fully mixed) due to the perturbing interaction. This is simulated in figure 13 and explains the origin of the name Level Mixing Resonances.

In reference 47 a detailed description of several features of this LM Resonances is given. For example it is shown that the non-diagonal matrix elements show a resonant dispersive character. Each of these resonances can be detected in the angular distribution, if the proper configuration is chosen.

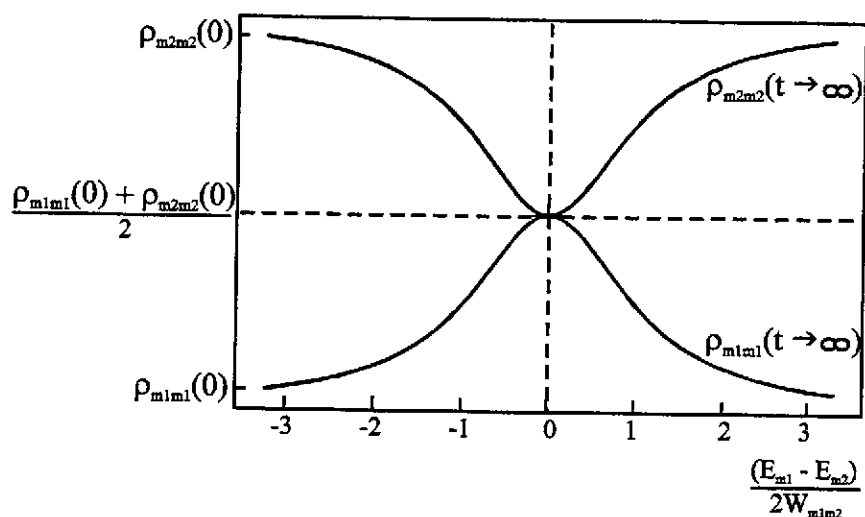


Figure 13: Simulation of the population probability of a pair of mixed levels for which the Level Mixing condition is fulfilled. In the resonance center, the two level populations are equalized. The resonance position is determined by the nuclear moment ratio.

#### IV.2. Perturbation of the nuclear orientation by the level mixing interaction:

##### the perturbation factor

To introduce the orientation described by this perturbed density matrix into the angular distribution, we need to use the relation between the density matrix and the density tensor (1). We also need to specify first the initial orientation more explicitly.

For this, we will discuss the example of nuclei that are produced in a fragmentation reaction. By selecting nuclei in the forward direction with respect to the primary beam, an ensemble of spin-aligned projectile fragments is obtained (with the alignment symmetry axis parallel to the beam axis)<sup>25)</sup>. During passage through the recoil spectrometer, the dipole fields will induce a rotation of the orientation axis, such that after the spectrometer the alignment axis is no more parallel to the secondary beam axis<sup>38)</sup>. To describe the initial alignment of the ensemble by one parameter  $B_2^0 \sim A$  (assuming we can restrict to second order tensor components in the angular distribution), we need to define a reference frame with the Z-axis parallel to the axial symmetry axis of the alignment ( $Z_{or}$  in fig. 10). This OR-axis system is defined with respect to an axis system fixed to an applied static magnetic field and the secondary beam direction (LAB-system, fig. 10). The LAB-system is rotating into the OR-system by rotation over the Euler angles  $(\gamma, \epsilon, 0)$ . For projectile fragments behind a doubly-achromatic

dipole spectrometer (like LISE at GANIL), the alignment axis is laying into the (X,Y)-plane and thus  $\varepsilon=90^\circ$ . Using the definition of tensor rotation <sup>12)</sup> we can then calculate the initial orientation tensor components in the LAB-frame, knowing that in the OR-frame the tensor has only one non-zero component ( $n'=0$ ):

$$\begin{aligned} B_2^n(t=0)_{LAB} &= \sum_{n'} D_2^{n'n}(0, -90, -\gamma) B_2^{n'}(t=0)_{OR} \\ &= e^{in\gamma} \sqrt{\frac{4\pi}{5}} Y_2^n(-90, 0) B_2^0(t=0)_{OR} \end{aligned} \quad (31)$$

In section II.4 we have already seen that the perturbed orientation tensor  $B_k^n(\tau)$  can be written as a product of a perturbation factors  $G_{kk'}^{nn'}$  and the initial orientation tensor  $B_k^{n'}(t=0)$ :

$$B_k^n(I, \omega_L, \omega_Q, \tau) = \sum_{k,n} G_{kk'}^{nn'}(I, \omega_L, \omega_Q, \tau) B_k^{n'}(I, t=0) \quad (32)$$

To derive an explicit expression for the perturbation factors, it is sufficient to transform expression (28) in its tensor form and to compare this with (32). The time integrated G-factors are given by:

$$G_{kk'}^{nn'}(\tau) = \hat{k}\hat{k}' \sum_{\substack{m,\mu \\ N,N'}} (-1)^{m-\mu} \begin{pmatrix} I & I & k \\ -m & m' & n \end{pmatrix} \begin{pmatrix} I & I & k' \\ -\mu & \mu' & n' \end{pmatrix} \langle m|N\rangle \langle N'|m\rangle \langle \mu|N\rangle^* \langle N'|\mu\rangle^* \frac{1-i\omega_{NN'}\tau}{1+(\omega_{NN'}\tau)^2} \quad (33)$$

If the Hamiltonian is described in the LAB system, the perturbation factor is calculated in the LAB-frame by determining the eigenstates and eigenfunctions of H numerically. In that case, the perturbed orientation tensor in (32) is also obtained in the LAB frame and the initial orientation tensor needs to be calculated also in this axis system (as given in (31)). Introduction of all these functions into the angular distribution function allows numerical calculations of the decay anisotropy as a function of the magnetic field strength.

If the Hamiltonian is expressed in the PAS-system (for example in case the two-level approximation is used), we can calculate an explicit analytical expression for the perturbation factors in the PAS-system by introducing the mixed eigenstates (22) and eigenvalues (23) from the perturbation theory approximation. In this case several types of perturbation factors can be distinguished. They are described in detail in the PhD thesis of P. Put <sup>61)</sup>, as well as in reference 45. The perturbation factor

approach is another mathematical formalism to describe the resonances, and more useful for numerical calculations of LMR.

### **IV.3. A typical feature of LMR: transfer of alignment into polarization**

In figure 14 we explain in a hand-waving way a typical feature of Level Mixing, which will have some important consequences for the study of exotic ground state moments. Assume that an ensemble of exotic nuclei is produced in such a way that its spins are aligned. This is for example the case for nuclei produced in projectile fragmentation, and selected in the forward direction (and thus with highest yield). No asymmetry can be detected in the  $\beta$ -decay of such an ensemble, because no spin-polarization is present. The only possibility to study the nuclear moments of  $\beta$ -decaying nuclei by measuring a resonance in the  $\beta$ -asymmetry, is either by producing a spin-polarized ensemble or by inducing the polarization via a hyperfine interaction.

To produce a spin-polarized ensemble of projectile fragments, the primary beam needs to be deflected to allow asymmetric selection of the secondary beam <sup>22,62,63)</sup>, and thus one obtains a reduction in the production yield. For the study of very exotic nuclei far from stability, where production rate becomes a limiting factor, efficient use of the forward selected highest fragment rate is necessary.

In these cases, it can be advantageous to use a measuring technique that allows inducing spin-polarization, starting from an initially aligned ensemble. This is not possible with the classical methods like NMR or NQR. But it is possible with LMR as illustrated in figure 14 for the simple case of a nucleus with spin  $I=1$ . Due to the combination of a quadrupole and a magnetic interaction, the level splitting between two hyperfine levels is not equidistant, and level crossings occur as a function of the magnetic field strength. We have seen in previous section that near the level crossing, the level populations of the  $m=0$  and  $m=1$  levels get mixed if the quadrupole and magnetic interaction are not perfectly collinear. Due to this mixing, an initially aligned ensemble is no longer aligned but polarized:  $p(1)$  and  $p(-1)$  are no longer equal. It is thus possible to induce spin-polarization, and thus measure an onset of  $\beta$ -asymmetry in the LMR.

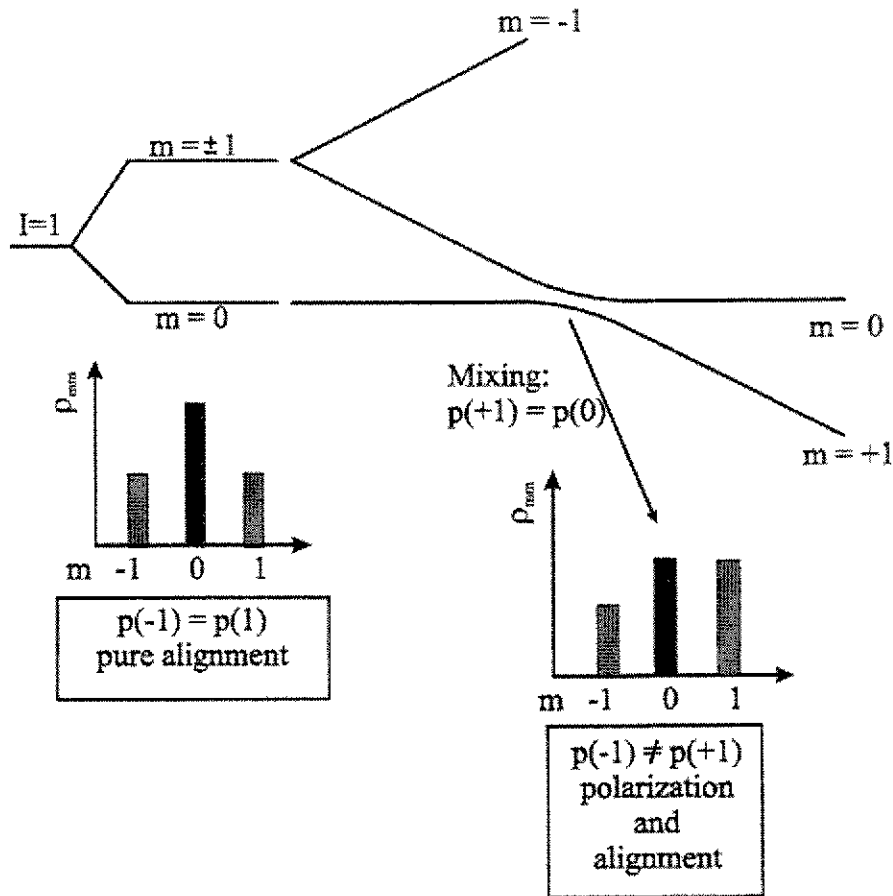


Figure 14: An initially aligned ensemble of nuclei with  $p(1)=p(-1)$  gets resonantly polarized due to the level mixing interaction that equalizes the mixing level populations. The onset of polarization occurs at a well defined value for the magnetic field, from which the nuclear moment ratio can be deduced.

The onset of polarization in a LMR of initially aligned  $\beta$ -decaying nuclei can be seen in the expression for the angular distribution by writing the  $B_1^0(\tau)$  density tensor in expression (12) explicitly as a function of the mixing density matrix elements:

$$W(\theta, \tau) = 1 - \sqrt{\frac{3}{2}} A_1 [\rho_{11}(\tau) - \rho_{-1,-1}(\tau)] \cos \theta \quad (34)$$

This is only an exact expression for the angular distribution in case of a nucleus with  $I=1$ , for which only one mixing occurs. For higher spin nuclei (34) is an approximation that needs to be interpreted with care. In the two-level approximation, the levels with  $m=0$  and  $m=1$  are getting mixed (fig. 14), while the population probability of the  $m=-1$  level is not modified by the interaction:

$$\rho_{-1,-1}(\tau) = \rho_{-1,-1}(0) \quad (35)$$



The asymmetry in the  $\beta$ -decay, defined as the difference between the detected electron intensity at 0 and 180 degrees with respect to the Z-axis, is thus proportional to the difference in the population probability of the  $m=1$  level before and after the level mixing interaction:

$$\begin{aligned} W(0, \tau) - W(180, \tau) &= -\sqrt{\frac{3}{2}} A_1 [\rho_{11}(\tau) - \rho_{11}(0)] \\ &= \sqrt{\frac{3}{8}} A_1 [\rho_{11}(0) - \rho_{00}(0)] L_{10}\left(\tau, \frac{E_1 - E_0}{2W_{10}}\right) \end{aligned} \quad (36)$$

Using expression (29) we find that the asymmetry is proportional to the initial population difference between the mixing  $m=0$  and  $m=1$  levels. This shows that even if only alignment is present, and  $p(1)=p(-1)$ , it is still possible to measure an asymmetry in the LMR.

## V. CONCLUSION

In this course we have given a few examples of hyperfine interaction methods that allow measuring the nuclear magnetic and quadrupole moment of short-lived nuclei or isomers. The typical regions of applicability of each of the methods has been discussed, and some examples have been given.

In the second section of the course, the mathematical formalism to describe the resonances due to the nuclear level mixing interaction has been derived. Some features of the resonances are discussed. The formalism has recently been further developed to include also the NMR interaction. An approximate solution is described in reference 55, and an exact solution will be published in near future.

I did not include experimental examples in this notes, because they can be found in several publications, as given in the reference list and mentioned at several places in the text.

## REFERENCES

- 1) Proc. Int. Conf. On « Nuclear Moments and Nuclear Structure », 1972, Physical Society of Japan, Ed. H. Horis, K. Sugimoto
- 2) H.E. Mahnke, Hyp. Int. 34 (1987) 47, G. Neyens et al., Nucl. Phys. A625 (1997) 668

- 3) I. Tanihata et al., Proc. 1st Int. Conf. On Radioactive Nuclear Beams 1989, Ed. W.D. Myers, J.M. Nitschke, E.B. Norman, World Scientific, p. 429
- 4) T. Motobayashi et al., Phys. Lett. B346 (1995) 9, E. Caurier et al., Phys. Rev. C 58 (1998) 2033
- 5) R. Broda et al., Phys. Rev. Lett. 74 (1995) 868, R. Grzywacz et al., Phys. Rev. Lett. 81 (1998) 766
- 6) H. Morinaga and T. Yamazaki, In beam Gamma-Ray Spectroscopy, North Holland Publishing Company (Amsterdam, New York, Oxford), 1976
- 7) Proc. 13th Int. Conf. On Electromagnetic Isotope Separators (EMIS), Eds. G. Munzenberg, H. Geissel, C. Scheidenberger, 1997
- 8) B.M. Sherrill, Proc. of the 2<sup>nd</sup> Radioactive Nuclear Beam conference 1991, Ed. Th. Delbar
- 9) R. Grzywacz et al., Phys. Lett. B 355 (1995) 439
- 10) M. Hass et al., Proc. 1st Int. Conf. On Radioactive Nuclear Beams, Ed. W. Myers, J.M. Nitschke, E. B. Norman, World Scientific, p.193
- 11) R.M. Steffen and K. Alder, "The Electromagnetic Interaction in Nuclear Spectroscopy" (North Holland, Amsterdam, 1975) 505
- 12) D.M. Brink and G.R. Satchler, Angular Momentum, Clarendon Press (Oxford), 1961
- 13) "Low Temperature Nuclear Orientation", Eds. Postma and N.J. Stone, North Holland (Amsterdam), 1986
- 14) C. Wu et al., Phys. Rev. C105 (1957) 1413
- 15) F.D. Correll et al., Phys. Rev. C 28 (1983) 862
- 16) M. Lindroos et al., Nucl. Instr. And Meth. In Phys. Res. A361 (1995) 53
- 17) U. Kopf et al., Z. Phys. 226 (1969) 297, E. Arnold et al., Phys. Lett. B. 197 (1987) 311
- 18) E. Arnold et al., Z. Phys. A 331 (1988) 295
- 19) P.A. Butler and P.J. Nolan, Nucl. Instr. And Meth. 190 (1981)283
- 20) H. Morinaga and T. Yamazaki, "In-beam gamma-ray spectroscopy", 1976
- 21) K. Asahi et al., Phys. Rev. C43 (1991) 456
- 22) K. Asahi et al., Phys. Lett. B 251 (1990) 488
- 23) H. Ueno et al., Phys. Rev. C53 (1996) 2142
- 24) P.F. Mantica et al., Phys. Rev. C55 (1997) 2501
- 25) G. Neyens et al., Phys. Lett. B393 (1997) 36
- 26) M. Schafer et al., Phys. Rev. C 57 (1998) 2205

- 27) E. Matthias et al., Phys. Rev. A4 (1971) 1626
- 28) E.N. Kaufmann, R.J. Vianden, Rev. Mod. Phys. 51 (1979) 161
- 29) M. Keim et al., Hyp. Int. 97/98 (1995) 543, E. Arnold et al., Phys. Lett. B(1992) 16
- 30) K.L.G Heyde, The Nuclear Shell Model, Springer-Verlag, Berlin Heidelberg, New York, London, Paris, Tokyo, Hong Kong, Barcelona, 1990
- 31) T. Minamisono et al., Phys. Rev. Lett. 69 (1992) 2058.
- 32) A. Iordachescu et al., Phys. Lett. B48 (1974) 28
- 33) R. Brenn et al., Nucl. Phys. A265 (1976) 35
- 34) K. Bonde Nielsen et al., J. Phys. C17 (1984) 3519
- 35) W.D. Schmidt-Ott et al., Z. Phys. A350 (1994) 215
- 36) G. Neyens and M. Hass, GANIL proposal E322 (PAC january 1999)
- 37) G. Goldring and M. Hass, Treatise on Heavy Ion Science, Ed. DA. Bromley, Vol3, 539
- 38) G. Neyens et al., Nucl. Instr. And Meth. In Phys. Res. A340 (94) 555-563
- 39) T. Minamisono et al., Nucl. Phys. A516 (1990) 365
- 40) H. Izumi et al., Phys. Lett. B366 (1996) 51
- 41) I.I. Sobelman, "Atomic Spectra and Radiative Transitions" (Springer-Verlag, Berlin, Heidelberg, New York, 1979)
- 42) E. Matthias et al, Phys. Rev. 125 (1962) 261
- 43) I. Tanihata et al., Physics Letters 67B (1977) 392
- 44) S. Shibuya et al., Hyp. Int. 14 (1983) 315
- 45) R. Coussement et al., Hyp. Int. 23 (1985) 273
- 46) P. Put et al., Hyp. Int. 22 (1985) 131
- 47) G. Scheveneels et al., Hyp. Int. 52 (1989) 257
- 48) R. Coussement et al., Phys. Lett. 97A (1983) 301
- 49) P. Put et al., Phys. Lett. 103A (1984) 151
- 50) F. Hardeman et al., Hyp. Int. 59 (1990) 13
- 51) F. Hardeman et al., Phys. Rev. C43 (1991) 130, G. Scheveneels et al., Phys. Rev. C43 (91) 2560,2566
- 52) F. Hardeman et al., Phys. Rev. C43 (1991) 514
- 53) G. Neyens et al., Nucl. Phys. A 555 (1993) 629-642

- 54) G. Neyens et al., Nucl. Instr. And Meth. A 340 (1994) 555-563
- 55) N. Coulier et al., Phys. Rev. C 59 (1999) 1935
- 56) G. Neyens et al., Physical Review Letters 82 (1999) 497-500
- 57) G. Goldring and M. Hass, Treaties on Heavy Ion Science, Ed. D.A. Bromley (Plenum Press) Vol. 3, p 539, C.P. Slichter in "Principles of Magnetic Resonance", eds. M. Cardona, P. Fulde, H.-J. Queisser (Springer-Verlag, Berlin, Heidelberg, New York, 1978)
- 58) D. Riegel, Physica Scripta 11 (1975) 228, G. Neyens et al., Phys. Rev. C 49 (1994) 645-649
- 59) K. Korringa, Physica XVI (1950) 601
- 60) Any basic quantum mechanics book, ex. S. Gasiorowicz, Quantum Physics, John Wiley & Son, New York, Chichester, Brisbane, Toronto, Singapore, 1974
- 61) P. Put, Ph. D. thesis University of Leuven, 1986, unpublished
- 62) K. Asahi et al., Nuclear Physics A588 (1995) 135c
- 63) K. Asahi et al., Proc. Second Int. Conf. On Radioactive Nuclear Beams, LLN, 1991